A&A 431, 197–202 (2005)
DOI: 10.1051/0004-6361:20041552

Astronomy & Astrophysics

The unidentified TeV source (TeV J2032+4130) and surrounding field: Final HEGRA IACT-System results

F. Aharonian[1], A. Akhperjanian[7], M. Beilicke[4], K. Bernlöhr[1], H.-G. Börst[5], H. Bojahr[6], O. Bolz[1], T. Coarasa[2], J. Contreras[3], J. Cortina[10], S. Denninghoff[2], V. Fonseca[3], M. Girma[1], N. Götting[4], G. Heinzelmann[4], G. Hermann[1], A. Heusler[1], W. Hofmann[1], D. Horns[1], I. Jung[1,9], R. Kankanyan[1], M. Kestel[2], A. Kohnle[1], A. Konopelko[1,14], D. Kranich[2], H. Lampeitl[4], M. Lopez[3], E. Lorenz[2], F. Lucarelli[3], O. Mang[5], D. Mazin[2], H. Meyer[6], R. Mirzoyan[2], A. Moralejo[3], E. Oña-Wilhelmi[3], M. Panter[1], A. Plyasheshnikov[1,8], G. Pühlhofer[11], R. de los Reyes[3], W. Rhode[6], J. Ripken[4], G. P. Rowell[1], V. Sahakian[7], M. Samorski[5], M. Schilling[5], M. Siems[5], D. Sobzynska[2,12], W. Stamm[5], M. Tluczykont[4,13], V. Vitale[2], H. J. Völk[1], C. A. Wiedner[1], and W. Wittek[2]

[1] Max-Planck-Institut für Kernphysik, Postfach 103980, 69029 Heidelberg, Germany
e-mail: [Gavin.Rowell;Dieter.Horns]@mpi-hd.mpg.de
[2] Max-Planck-Institut für Physik, Föhringer Ring 6, 80805 München, Germany
[3] Universidad Complutense, Facultad de Ciencias Físicas, Ciudad Universitaria, 28040 Madrid, Spain
[4] Universität Hamburg, Institut für Experimentalphysik, Luruper Chaussee 149, 22761 Hamburg, Germany
[5] Universität Kiel, Inst. f. Experimentelle und Angewandte Physik, Leibnizstr. 15-19, 24118 Kiel, Germany
[6] Universität Wuppertal, Fachbereich Physik, Gaußstr. 20, 42097 Wuppertal, Germany
[7] Yerevan Physics Institute, Alikhanian Br. 2, 375036 Yerevan, Armenia
[8] Altai State University, Dimitrov Street 66, 656099 Barnaul, Russia
[9] Now at Washington University, St. Louis MO 63130, USA
[10] Now at Max-Planck-Institut für Physik, Föhringer Ring 6, 80805 München, Germany
[11] Now at Landessternwarte Heidelberg, Königstuhl, 69117 Heidelberg, Germany
[12] Home institute: University Lodz, Poland
[13] Now at Laboratoire Leprince-Ringuet, École Polytechnique, 91128 Palaiseau, France (IN2P3/CNRS)
[14] Now at Humboldt Universität f. Physik, Unter den Linden 6, 10099 Berlin, Germany

Received 29 June 2004 / Accepted 17 September 2004

Abstract. The unidentified TeV source in Cygnus is now confirmed by follow-up observations from 2002 with the HEGRA stereoscopic system of Cherenkov Telescopes. Using all data (1999 to 2002) we confirm this new source as steady in flux over the four years of data taking, extended with radius 6.2′ ($\pm 1.2'_{\rm stat} \pm 0.9'_{\rm sys}$) and exhibiting a hard spectrum with photon index −1.9. It is located in the direction of the dense OB stellar association, Cygnus OB2. Its integral flux above energies $E > 1$ TeV amounts to ∼5% of the Crab assuming a Gaussian profile for the intrinsic source morphology. There is no obvious counterpart at radio, optical nor X-ray energies, leaving TeV J2032+4130 presently unidentified. Observational parameters of this source are updated here and some astrophysical discussion is provided. Also included are upper limits for a number of other interesting sources in the FoV, including the famous microquasar Cygnus X-3.

Key words. gamma rays: observations – stars: early-type – open clusters and associations: individual: Cygnus OB2

1. Introduction

The reasonably large fields of view (FoV, e.g. $FWHM \geq 3°$) achieved by ground-based γ-ray telescopes permits survey-type observations using a few or even singly pointed observations. Such potential was realised with the serendipitous discovery of a TeV source in the Cygnus region. Analysis of archival data (∼121 h from 1999 to 2001) of the HEGRA system of Imaging Atmospheric Cherenkov Telescopes (HEGRA IACT-System) revealed convincing evidence for an apparently steady, spectrally hard (−1.9 differential photon index) and possibly extended TeV source (Aharonian et al. 2002). Follow-up observations using the HEGRA IACT-System were performed during its final season of operation (2002) for a total of ∼158 h. Analysis of these data again reveal the presence of this source, thus confirming its existence with the HEGRA IACT-System. Earlier, observations (1991) with the HEGRA scintillator array (Merck 1993) revealed a multi-TeV excess, positionally consistent with Cygnus X-3. Analysis with improved direction reconstruction (Krawczynski 1995) revealed this excess ($+4.3\sigma$ pre-trial) as centered roughly 0.5° north of Cygnus X-3. Interestingly, the Crimean group (using the

Cherenkov imaging technique) reported a significant excess ($\sim+6.0\sigma$ pre-trial) $\sim0.7^\circ$ north of Cygnus X-3 (Neshpor et al. 1995), and recently, the Whipple collaboration also reported an excess at the HEGRA position ($+3.3\sigma$) in their archival data of 1989/1990 (Lang et al. 2004).

We summarise here in some detail our analysis and numerical results for TeV J2032+4130, and give a brief astrophysical interpretation. Given the large FoV of observations, deep exposures were also obtained for a number of other interesting sources. Upper limits for these sources are given.

2. Data analysis & results

The HEGRA IACT-System, de-commissioned in September 2002, consisted of five identical Cherenkov telescopes (each with 8.5 m^2 mirror area) on the Canary Island of La Palma (2200 m a.s.l.). Employing the stereoscopic technique, this system achieved an angular resolution $<0.1^\circ$ and energy resolution <15% for γ-rays on an event-by-event basis over the 0.5 TeV to >50 TeV regime. Detailed technical descriptions of the HEGRA IACT-System and performance can be found in Pühlhofer et al. (2003).

Gamma-ray-like events are preferentially selected against those of the dominant isotropic background of cosmic-rays (CR). This is achieved with cuts on θ, the angular distance between the reconstructed and assumed arrival directions, and also the *mean-scaled-width* $\bar{w}$ (Aharonian et al. 2000a), which is a measure of an image's conformity to a γ-ray-like shape. Event arrival directions are reconstructed using the algorithms described in Hofmann et al. (1999). We a priori selected algorithm "3" for final analysis, but also employed the other available algorithms to check consistency of the signal. So-called *tight cuts* were implemented, namely: $\theta < 0.12^\circ$, $\bar{w} < 1.1$, which are optimal for point-like sources in a background-dominated scenario. We also required a minimum $n_{\rm tel} \geq 3$ telescope images per event for the θ and $\bar{w}$ calculation (Aharonian et al. 2002). An estimate of the CR background surviving cuts is made using both the template (see Rowell 2003) and displaced background models for consistency checks on the source excess. The displacement background model employs different regions in the FoV for background estimation using events from $\bar{w} < 1.1$.

In Tables 1 and 2 we summarise details of the TeV source which includes the excess significance, the source extension $\sigma_{\rm src}$, both of which are calculated at the excess centre of gravity (CoG), and also the energy spectrum and flux. Some results are split according to data subsets, 1999 to 2001 (dataset §1), and 2002 (dataset §2).

The CoG and source extension were estimated by fitting a 2D Gaussian convolved with the system point spread function (PSF) to a histogram of γ-ray-like ($\bar{w} < 1.1$) events binned over a $1^\circ \times 1^\circ$ FoV. The PSF is estimated from Crab data, giving a value which agrees with Monto Carlo simulations of a point source (Aharonian et al. 2000b, 2004). A Gaussian profile suitably describes the excess morphology (discussed later). Here, we used higher quality events selected according to the estimated error in reconstructed direction ϵ (see e.g. Hofmann et al. 2000a). This cut on ϵ reduced somewhat the systematic differences in CoG obtained from all three available algorithms "1", "2" and "3". Simulations and empirical results from other point sources of the HEGRA IACT-System archive have shown that consistent sensitivities from all algorithms are expected for a minimum number of images per event $n_{\rm tel} \geq 3$. In fact the signal excess significance from all data using each algorithm are consistent to within 1σ, and the CoGs and source extensions agree to within a 2σ level. Taking the final CoG and source extension from algorithm "3", the respective systematic errors were taken using results from the other algorithms. The excess significance from combined data exceeds

Table 1. Numerical summary for TeV J2032+4130. **a)** Centre of Gravity (CoG) and extension $\sigma_{\rm src}$ (std. dev. of a 2D Gaussian); **b)** event summary. The values s and b are event numbers for the γ-ray-like and background (from the Template and Displaced models, see text) respectively, and $s - \alpha b$ is the excess using a normalisation α. S denotes the excess significance using Eq. (17) of Li & Ma (1983); **c)** integral events after spectral cuts.

(a) CoG & Extension ($\epsilon \leq 0.12^\circ$)

— All Data (278.3 h) —		
RA α_{2000}:	$20^{\rm hr}\ 31^{\rm m}\ 57.0^{\rm s}$	$\pm6.2^{\rm s}_{\rm stat}\ \pm13.7^{\rm s}_{\rm sys}$
Dec δ_{2000}:	$41^\circ\ 29'\ 56.8''$	$\pm1.1'_{\rm stat}\ \pm1.0'_{\rm sys}$
$\sigma_{\rm src}$	$6.2'$	$\pm1.2'_{\rm stat}\ \pm0.9'_{\rm sys}$

(b) Tight cuts: $\theta < 0.12^\circ$, $\bar{w} < 1.1$, $n_{\rm tel} \geq 3$

Background model	s	b	α	$s - \alpha b$	S
— 1999 to 2001 Dataset §1 (120.5 h) —					
Template	529	2432	0.168	123	**+5.3**
Displaced	529	6982	0.059	119	**+5.4**
— 2002 Dataset §2 (157.8 h) —					
Template	716	3494	0.168	129	**+4.8**
Displaced	716	8510	0.070	125	**+4.8**
— All Data (278.3 h) —					
Template	1245	5926	0.168	252	**+7.1**
Displaced	1245	15492	0.065	243	**+7.1**

(c) Spectral Cuts: Tight Cuts + core ≤ 200 m

Energy estimation method: See Hofmann et al. (2000b)

Background model	s	b	α	$s - \alpha b$	S
— 1999 to 2001 Dataset §1 (120.5 h) —					
Displaced	421	2120	0.143	118	**+6.0**
— 2002 Dataset §2 (157.8 h) —					
Displaced	552	2999	0.143	124	**+5.3**
— All Data (278.3 h) —					
Displaced	973	5119	0.143	242	**+7.9**

Table 2. Numerical summary for TeV J2032+4130 continued.. **d)** differential fluxes and events after tight spectral cuts; **e)** fitted power law; **f)** integral flux.

(d) Spectral Cuts: Differential points

Energy E(TeV)	Flux $(E)^a$	Flux^a Error(E)	s	b	S^b
— 1999 to 2001 Dataset §1 (120.5 h) —					
1.05	1.70	1.24	130	678	**+3.0**
1.82	1.94	0.91	107	531	**+3.1**
3.16	0.37	0.27	57	323	**+1.4**
5.50	0.30	0.11	33	117	**+3.2**
9.55	0.09	0.04	13	34	**+2.8**
— 2002 Dataset §2 (157.8 h) —					
1.05	19.90	16.57	153	885	**+2.1**
1.82	1.85	1.56	152	913	**+1.7**
3.16	0.85	0.28	107	513	**+3.4**
5.50	0.28	0.10	44	174	**+3.2**
9.55	0.07	0.04	17	51	**+2.8**
— All Data (278.3 h) —					
1.05	11.98	10.80	283	1563	**+3.6**
1.82	1.89	0.97	259	1444	**+3.3**
3.16	0.64	0.20	164	836	**+3.6**
5.50	0.29	0.07	77	291	**+4.5**
9.55	0.08	0.03	30	85	**+3.9**

[a] Flux and Errors in units $\times 10^{-13}$ ph cm^{-2} s^{-1} TeV^{-1}.
[b] Significance from Li & Ma (1983) Eq. (17) using s, b and a normalisation $\alpha = 0.143$.

(e) Fitted Spectrum: Pure Power-Law

$\mathrm{d}N/\mathrm{d}E$	=	$N\ (E/1\,\mathrm{TeV})^{-\gamma}$ ph cm^{-2} s^{-1} TeV^{-1}
— 1999 to 2001 Dataset §1 (120.5 h) —		
N	=	$4.1\ (\pm 2.1_{\mathrm{stat}} \pm 1.3_{\mathrm{sys}}) \times 10^{-13}$
γ	=	$1.7\ (\pm 0.3_{\mathrm{stat}} \pm 0.3_{\mathrm{sys}})$
— 2002 Dataset §2 (157.8 h) —		
N	=	$9.3\ (\pm 2.9_{\mathrm{stat}} \pm 1.4_{\mathrm{sys}}) \times 10^{-13}$
γ	=	$2.1\ (\pm 0.2_{\mathrm{stat}} \pm 0.3_{\mathrm{sys}})$
— All Data (278.3 h) —		
N	=	$6.2\ (\pm 1.5_{\mathrm{stat}} \pm 1.3_{\mathrm{sys}}) \times 10^{-13}$
γ	=	$1.9\ (\pm 0.1_{\mathrm{stat}} \pm 0.3_{\mathrm{sys}})$

(f) Integral Flux^a (E > 1 TeV)

— 1999 to 2001 Dataset §1 (120.5 h) —		
$F(E > 1\,\mathrm{TeV})$	=	$5.86\ (\pm 3.91_{\mathrm{stat}})$
— 2002 Dataset §2 (157.8 h) —		
$F(E > 1\,\mathrm{TeV})$	=	$8.45\ (\pm 3.05_{\mathrm{stat}})$
— All Data (278.3 h) —		
$F(E > 1\,\mathrm{TeV})$	=	$6.89\ (\pm 1.83_{\mathrm{stat}})$

[a] Flux and Errors in units $\times 10^{-13}$ ph cm^{-2} s^{-1}.

7σ ($+7.1\sigma$), and the source appears extended at the $>4\sigma$ level when, conservatively, subtracting the systematic error in extension. The source is termed TeV J2032+4130 based on its CoG. The post-trial significance is $\sim 6.1\sigma$ if one assumes the trial factors (1100) accrued from the discovery dataset §1 (Aharonian et al. 2002). The radial source extension is shown in Fig. 1 and compared against a number of possible source morphologies. We tested three different types of intrinsic source morphology:

- Disc: the source emits at a constant brightness out to a radius 0.13° (with zero brightness outside). This profile resembles that of a disc.
- Volume: the source emits at all positions inside a sphere of radius 0.13°.
- Surface: the source emits at all positions within a radial band between 0.117° and 0.13°.

In each case the volume-integrated radial brightness is calculated after convolution with the instrument PSF, and compared with the measured radial profile of TeV J2032+4130. In all cases similar reduced-χ^2 ~1.0 were obtained, thereby not permitting discrimination between these source morphologies.

Figure 2 depicts the 2D *skymap* of excess significance over the FoV, using the template model as a CR background estimate. TeV J2032+4130 is clearly positioned at the edge of the error circle of 3EG J2033+4118, and within the core circle of the extremely dense OB stellar association Cygnus OB2 (Knödlseder 2000).

The energy spectrum determination followed the method described in Aharonian et al. (1999) using tight cuts (on θ and $\bar{w}$) plus an additional cut on the reconstructed air-shower core distance of the event core <200 m. Reconstruction of event energies employed the more advanced method of Hofmann et al. (2000b) which makes use of the height of shower maximum to improve the core distance determination, and hence improve energy resolution to <15%. Both datasets §1 and §2 yielded consistent power-law fits with a hard photon index. For all data, a pure power law explains well the energy spectrum, showing no indication for a cut-off when fitting also a combined power law + exponential cutoff term $\exp(-E/E_{\mathrm{c}})$. We estimated, nevertheless, lower limits (99% c.l.) to the cut-off energy for a range of (fixed) power law indices. Cut-off lower limits of $E_{\mathrm{c}} \sim 3.6, 4.2$ and 4.6 TeV result when fixing the power index at values $\gamma = 1.7$, 1.9, and 2.2, respectively.

In estimating all flux values we have assumed a Gaussian source profile according to the estimated source size since the non-pointlike nature of the source is confirmed. Note that previously published integral fluxes for combined data (Rowell et al. 2003; Horns et al. 2004) assumed a pointlike source. It is also apparent that the event rate for dataset §2 is ~80% that of dataset §1, and that the integral fluxes (for $E > 1$ TeV) derived differ by about 40%. However the statistical errors on the integral flux, which are dominated by contributions near 1 TeV, suggests this difference is not significant ($\sim 1\sigma$).

We conclude therefore that TeV J2032+4130 exhibited a constant flux from 1999 to 2002. Note that the integral (and differential) fluxes are corrected for changes in the IACT-System response over time (see Pühlhofer et al. 2003, for details on the system performance over time). In this case, corrections up to the individual run level according to the CR background rate

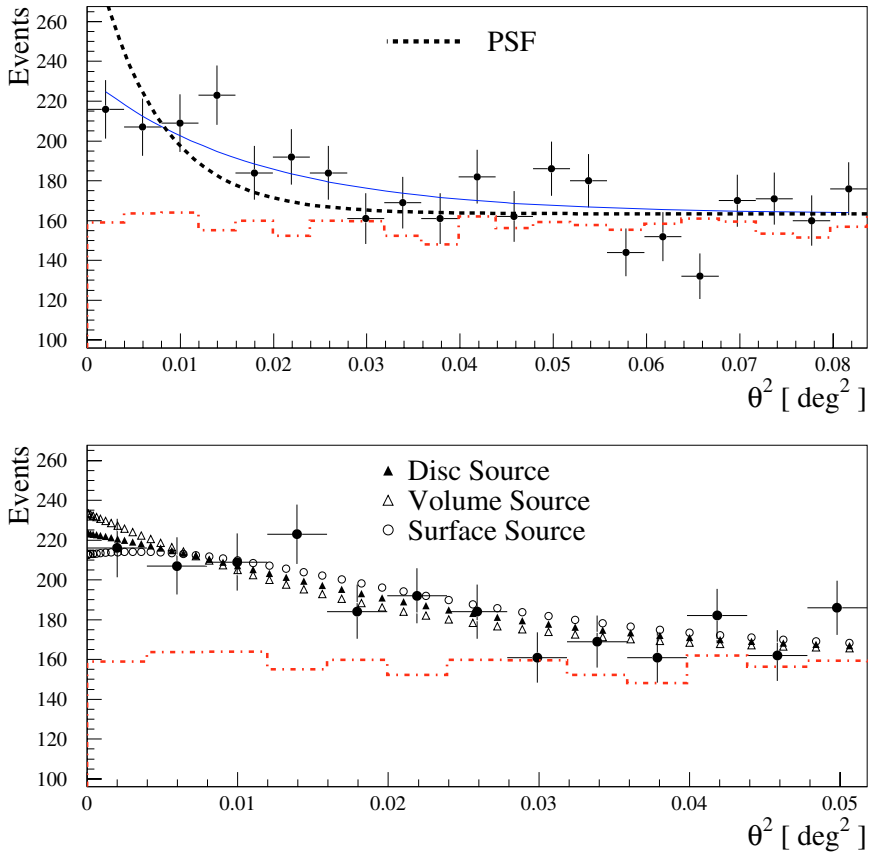

Fig. 1. (*Top*) Events (solid points with error bars) vs. distance from the CoG squared θ^2 compared with a background estimate from the template model (dashed-dotted line). A convolved radial Gaussian fit $F = Ped + P_2 \exp(-\theta^2/(P_1^2 + \sigma_{pt}^2))$ is indicated by the solid line with $P_1 = \sigma_{src} = 0.104^\circ \pm 0.020^\circ$ the intrinsic source size. The PSF width is $\sigma_{pt} = 0.070^\circ$ (dashed). The pedestal *Ped* is fitted separately. (*Bottom*) Comparisons with various intrinsic source morphologies convolved with the PSF (see text).

(a reliable, relative measure of the detector+atmospheric transmission) have been applied.

We also include in Table 3, 99% upper limits for a number of other interesting sources in the FoV. These include the two GeV sources, their possible associated X-ray counterparts (as indicated by Roberts et al. 2001), and also Cygnus X-3.

3. Discussion and conclusion

Possible origins of TeV J2032+4130 have been considered in Aharonian et al. (2002), Butt et al. (2003), Mukherjee et al. (2003) and Bednarek (2003). One interpretation involves association with the stellar winds of member stars in Cygnus OB2, individually or collectively, which provide conditions conducive to strong and stable shock formation for particle acceleration. Another scenario involves particle acceleration at a termination shock, which is expected at the boundary where a relativistic jet meets the interstellar medium. TeV J2032+4130 in fact aligns well within the northern error cone of the bi-lobal jet of Cygnus X-3 discussed by Martí et al. (2000, 2001). The existence of TeV emission clearly suggests that particles are accelerated to at least multi-TeV energies. Taken at face value the different flux levels (a maximum factor ~20 difference) claimed by the Crimean (1.7 Crab $E > 1$ TeV), HEGRA (0.05 Crab $E > 1$ TeV) and Whipple (0.12 Crab $E > 0.6$ TeV) groups over a period of a decade, would suggest episodic emission from TeV J2032+4130. Explaining also the extended nature of TeV J2032+4130 as seen by HEGRA requires consideration of issues such as the particle acceleration site and its distance to that of the TeV γ-ray emission, particle diffusion and source

Table 3. Summary of point-like flux upper limits for other sources in the FoV. Positions for the various X-ray sources are taken from Roberts et al. (2001). An energy threshold of $E_{th} > 0.7$ TeV is estimated based on the average zenith angle $\bar{z}$ of observations: $E_{th} = 0.5 \cos(\bar{z})^{-2.5}$. The template background model been used ($\alpha = 0.168$), with s, b and S defined as in Table 1.

Other Sources: (tight cuts) $\theta < 0.12^\circ$, $\bar{w} < 1.1$, $n_{tel} \geq 3$

Source	s	b	$s - \alpha\, b$	S	$^a\phi^{99\%}$
GeV J2026+4124	541	3429	−35	**−1.3**	**0.29**
AX J2027.6+4116	771	4497	16	**+0.6**	**0.42**
GeV J2035+4214	784	4457	35	**+1.2**	**0.45**
AX J2036.0+4218(Src1)	620	4005	−53	**−1.8**	**0.22**
AX J2035.4+4222(Src2)	663	4083	−23	**−0.7**	**0.27**
AX J2035.9+4229(Src3)	584	3626	−25	**−0.9**	**0.28**
Cygnus X-3	857	5613	−86	**−2.6**	**0.17**

$^a\,\phi_{ph}^{99\%}$ = 99% upper limit $E_{th} > 0.7$ TeV [$\times 10^{-12}$ ph cm^{-2} s^{-1}].

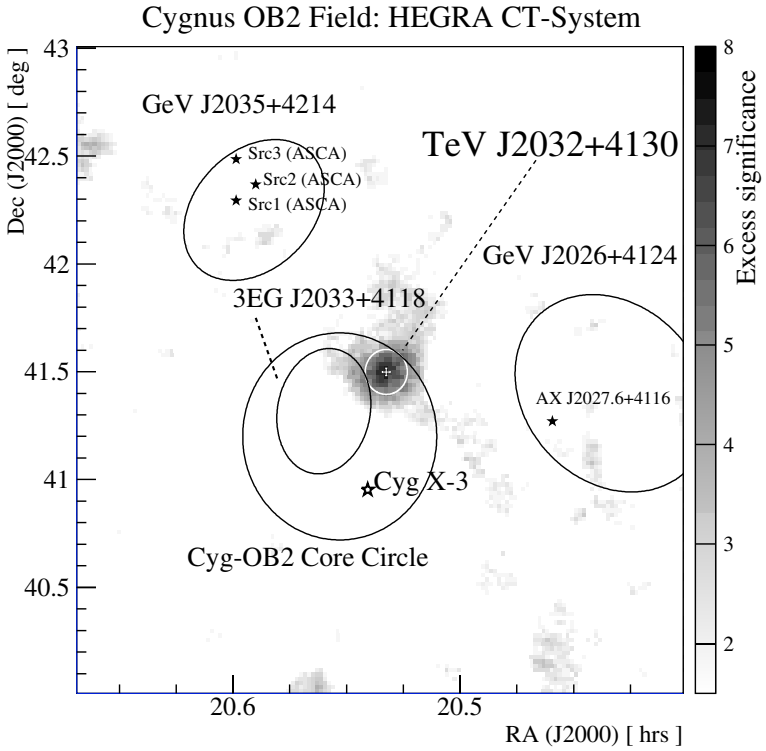

Fig. 2. Skymap of correlated event excess significance (σ) from all HEGRA IACT-System data (3.0° × 3.0° FoV) centred on TeV J2032+4130. Nearby objects are indicated (EGRET sources with 95% contours). The TeV source centre of gravity (CoG) with statistical errors, and intrinsic size (std. dev. of a 2D Gaussian, $\sigma_{\rm src}$) are indicated by the white cross and white circle, respectively.

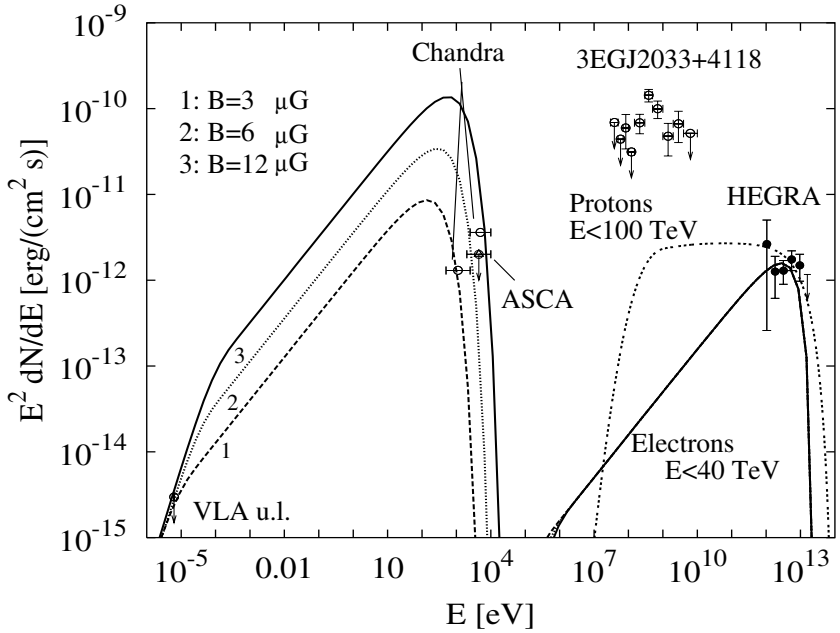

Fig. 3. Spectrum of TeV J2032+4130 (this work – HEGRA) compared with purely hadronic (Protons $E < 100$ TeV) and leptonic (Electrons $E < 40$ TeV) models. Upper limits, constraining the synchrotron emission (leptonic models), are from the VLA and *Chandra* (Butt et al. 2003) and ASCA (Aharonian et al. 2002). In the model a minimum electron energy $\gamma_{\rm min} \sim 10^4$ is chosen to meet the VLA upper limit. EGRET data points are from the 3rd EGRET catalogue (Hartman et al. 1999).

age. Such issues would also not in general rule out an extended *and* episodic source. Moreover the TeV J2032+4130 emission at any given time may be a superposition of more than one component (e.g. variable compact in addition to weak, steady, extended emission).

For illustrative purposes we have matched the spectral energy distribution of TeV J2032+4130 with simplistic leptonic and hadronic models (Fig. 3). We assume that the TeV emission arises from a single pure population of either non-thermal hadronic or electronic parent particles. We do not consider here

the conditions under which particles are accelerated or how they lose energy. Under the hadronic scenario the π°-decay prediction matches well the TeV flux using a parent proton power law spectrum of index −2.0 with a sharp limit at 100 TeV. The neighbouring EGRET source 3EG J2033+4118 (possibly not related to TeV J2032+4130) should be considered here as upper limits on the potential GeV flux of TeV J2032+4130. Associated synchrotron X-ray emission would also be expected from tertiary electrons ($\pi^{\pm} \ldots \rightarrow \mu^{\pm} \ldots \rightarrow e^{\pm}$), not modeled at present, which represent an absolute lower limit on any synchrotron emission visible assuming a pure electronic scenario. TeV data are matched well by an inverse-Compton spectrum (from electrons up-scattering the cosmic microwave background) arising from an electron spectrum with power law index ~ -2.0 and a sharp limit at 40 TeV. The predicted synchrotron emission then follows as a function of local magnetic field, constrained by the available upper limits at radio and X-ray energies. The most conservative synchrotron prediction arises for $B_0 = 3\ \mu$G, the lowest such B-field expected in the Galactic disk. In fact, much higher B-fields ($B_0 > 10\ \mu$G) are generally expected in such regions containing young/massive stars with high mass losses and colliding winds (e.g. Eichler et al. 1993). X-ray results from ASCA (Aharonian et al. 2002) provide constraining upper limits, as do results from *Chandra* (Butt et al. 2003). Deeper observations by XMM and *Chandra* will no doubt provide further constraints on the leptonic component. Future γ-ray observations by H.E.S.S., VERITAS and also MAGIC-II will be vital in better determining the spectrum over the ∼50 GeV to >10 TeV regime. Knowledge of the spectral behaviour for $E > 10$ TeV will convey important information on the maximum particle energies and their type. Such information can come from low elevation observations by H.E.S.S. for which very large collecting areas are achieved at TeV energies. Energy-resolved morphology studies can also be performed, allowing conclusions on the diffusion properties of the accelerated particles. Overall, TeV J2032+4130 is the only TeV source so far without an obvious multiwavelength counterpart, and is likely the first-discovered galactic TeV source which is extended in nature.

The serendipitous detection of such a weak (∼0.05 Crab), marginally extended source with a hard spectrum over a long observation time illustrates the power of the stereoscopic technique as was employed by the HEGRA IACT-System. With a sensitivity at least a factor of 5 better, the next generation instruments will find such sources detectable in under 10 h, or even less for sources with steeper energy spectra.

Finally, we also obtained upper limits (for a steady TeV flux) from a number of other source positions in the FoV (Fig. 2, Table 3), including the famous microquasar Cygnus X-3 for which an upper limit ($E > 0.7$ TeV) 1.7×10^{-13} ph cm^{-2} s^{-1} for steady emission is set.

Acknowledgements. The support of the German Ministry for Research and Technology BMBF and of the Spanish Research Council CICYT is gratefully acknowledged. We thank the Instituto de Astrofísica de Canarias for the use of the site and for supplying excellent working conditions at La Palma. We gratefully acknowledge the technical support staff of the Heidelberg, Kiel, Munich and Yerevan Institutes. GPR acknowledges receipt of a von Humboldt fellowship.

References

Aharonian, F. A., Akhperjanian, A. G, Barrio, J. A., et al. 1999, A&A, 349, 11
Aharonian, F. A., Akhperjanian, A. G., Barrio, J. A., et al. 2000a, ApJ, 539, 317
Aharonian, F. A, Akhperjanian, A. G., Barrio, J. A., et al. 2000b, A&A, 361, 1073
Aharonian, F. A., Akhperjanian, A., Beilicke, M., et al. 2002, A&A, 393, L37
Aharonian, F. A., Akhperjanian, A., Beilicke, M., et al. 2004, ApJ, in press [arXiv:astro-ph/0407118]
Bednarek, W. 2003, MNRAS, 345, 847
Butt, Y., Benaglia, P., Combi, J. A., et al. 2003, ApJ, 597, 494
Eichler, D., & Usov, V. 1993, ApJ, 402, 271
Hartman, R. C., Bertsch, D. L., Bloom, S. D., et al. 1999, ApJS, 123, 79
Hofmann, W., Jung, I., Konopelko, A., et al. 1999, Astropart. Phys., 10, 275
Hofmann, W., Akhperjanian, A. G, Barrio, J. A., et al. 2000a, A&A, 361, 1073
Hofmann, W., Lampeitl, H., Konopelko, A., et al. 2000b, Astropart. Phys., 12, 135
Horns, D., Rowell, G. P., et al. 2004, New AR, 48, 489
Knödlseder, J. 2000, A&A, 360, 539
Krawczynski, H. 1995, Diplom Thesis, University of Hamburg, Hamburg
http://www-hegra.desy.de/publications.html
Lang, M. J., Carter-Lewis, D. A., Fegan, D. J., et al. 2004, A&A, 423, 415
Li, T. P., & Ma, Y. Q. 1983, ApJ, 272, 317
Merck, M. 1993, Ph.D. Dissertation, Ludwig-Maximilians University, Munich
Martí, J., Paredes, J. M., Peracaula, M., et al. 2000, ApJ, 545, 939
Martí, J., Paredes, J. M., Peracaula, M., et al. 2001, A&A, 375, 476
Mukherjee, R., Halpern, J. P., Gotthelf, E. V., et al. 2003, ApJ, 589, 487
Neshpor, Y. I., Kalekin, O. R., Stepanian, A. A., et al. 1995, Proc. 24th ICRC (Rome), 2, 1385
Pühlhofer, G., Bolz, O., Götting, N., et al. 2003, Astropart. Phys., 20, 267
Roberts, S. E., Romani, R. W., & Kawai, N. 2001, ApJS, 133, 451
Rowell, G. P. 2003, A&A, 410, 389
Rowell, G. P., et al. 2003, Proc. 28th ICRC Tsukuba, OG 2.2, 2345 [arXiv:astro-ph/0307334]